

Quantum Logical Gates with Linear Quadripartite Cluster States of Continuous Variables

Aihong Tan Changde Xie* Kunchi Peng

(State Key Laboratory of Quantum Optics and Quantum Optics Devices, Institute of
Opto-Electronics, Shanxi University, Taiyuan 030006, People's Republic of China)

Abstract: The concrete schemes to realize three types of basic quantum logical gates using linear quadripartite cluster states of optical continuous variables are proposed. The influences of noises and finite squeezing on the computation precision are analyzed in terms of the fidelity of propagated quantum information through the continuous variable cluster states. The proposed schemes provide direct references for the design of experimental systems of one-way quantum computer based on the cluster entanglement of amplitude and phase quadratures of light.

1 Introduction

Quantum computer (QC) promises efficient processing of certain computational tasks that are intractable with classical computer technology. Most of the concepts of quantum information and computation have been generalized in continuous variables (CV) [1] after they were initially developed for discrete variables (DV) [2]. A universal DV QC can perform any desired unitary transformation over discrete quantum variables by local operations, which are implemented on sequences of unitary quantum logic gates. Being different from the widely used quantum circuit model of QC [3], a novel model of quantum computation based on a highly entangled cluster state was proposed by Rausserdorf and Briegel, in which the computation is completed only through single-qubit projective measurements [4]. Because of the essential role of measurement, the cluster based QC is irreversible, thus it was named the one-way QC [5]. The feasibility of one-way quantum computing has been experimentally demonstrated in single-photon regime with four-qubit cluster states [6-8].

In 1999, Lloyd and Braunstein provided necessary and sufficient conditions for constructing a universal CV QC and shown that QC over quadratures of the electromagnetic field might be realized using simple linearly optical elements such as beam splitters and phase shifters, together with squeezers of light and nonlinear devices[9]. As a new type of multipartite entanglement, the conception of qubit-based cluster state was extended to CV and it was claimed that such states may be applied in quantum network communication but cannot be used in universal QC over CV because of their Gaussian character [10]. Successively, a universal QC model with CV cluster states was proposed by Menicucci et al. as a generalization of DV QC cluster-state model [11]. It was pointed out in Ref.[11] that the universal one-way quantum computation based on CV cluster states can be performed only by adding to the toolbox (squeezed light, linear optics, and homodyne detection) any single-mode non-Gaussian measurement, while the initial cluster state itself remains Gaussian. In

the proposed optical implementation of universal QC model using CV cluster states, squeezed-light sources serve as the nodes of the cluster, thus not only computation can be performed deterministically, but also the preparation of CV cluster states can be done unconditionally[11, 12]. Although the optical modes of the electromagnetic field provide a suitably experimental test bed for demonstrating the general principles of cluster-based QC, there is no any experimental result to be presented so far. We consider that the absence of the concrete design on the experimental systems is one of the reasons limited the progress of CV QC experimental research. Quantum logical gates are the most basic computing devices in QC which perform elementary quantum operations. To prompt the experimental study on one-way QC based on CV cluster states of light, we propose the schemes to realize the single-mode and multi-mode Gaussian quantum logical operations using linear quadripartite cluster states of electromagnetic field, which have been experimentally prepared [13, 14]. In Ref.[12], Looock illustrated the principles of one-way QC using Gaussian CV cluster states with simple examples. Here, we will discuss concrete schemes for experimentally implementing quantum logical gates in one-way CV QC. The influences of the quantum noises and the finite squeezing of light on the computation precision will be analyzed in terms of fidelity of propagated quantum information through CV cluster states. Our analysis shows that finite squeezing reduces the precision of quantum logical operations. In practice, the ability of optical CV QC depends crucially on the squeezing degree of light used to prepare CV cluster states.

The paper is organized as follows: we simply describe the experimentally generating method of the quadripartite linear CV cluster states via the linearly optical transformation of a pair of two-mode squeezed states of light produced from two non-degenerate optical amplifiers (NOPAs) in the second section. Then we introduce the schemes to realize the phase-space displacement transformation, the single-mode squeezing operation and the CNOT operation using the cluster states in the sections 3 to 5, respectively. At last a brief conclusion is given in the section 6.

2 Preparation of quadripartite CV cluster states

The schematic diagram for the experimental generation of the quadripartite linear CV cluster states, which will be used in following schemes for quantum logical gates, is shown in Fig.1. As that detailedly described in Ref.[13], two phase-quadrature squeezed states(a_1^s, a_4^s) and two amplitude-quadrature squeezed states(a_2^s, a_3^s) are simultaneously produced from a pair of NOPAs(NOPA1 and NOPA2) which consists of a type-II χ^2 nonlinearly optical crystal and an optical resonator[15]. The pump laser is a frequency-doubled CW laser, the output harmonic wave of which is used for the pump fields of the two NOPAs and the subharmonic wave serves as the injected signals(a_{01}, a_{02}, a_{03} and a_{04}) of the NOPAs as well as the local oscillators(LO) in the homodyne detections(see Fig.2 and 6). The beam splitters used in this system are chosen to completely eliminate all anti-squeezing components [14]. We take 1:4 beam splitter for BS₁, and 50% beam splitters for BS₂ and BS₃. At first interfering modes a_2^s and a_3^s on BS₁ with the phase difference of $\pi/2$ to produce two output modes a_5 and a_6 , and then combining modes a_1^s and a_5 on BS₂ with the phase difference of 0 and combining modes a_4^s and a_6 on BS₃ with the phase difference of $\pi/2$, the final four output modes $b_i (i=1,2,3,4)$ are in the linear cluster state[10, 13, 14]. It has been theoretically [10] and experimentally [13, 14] demonstrated that if the correlation variances of the amplitude quadratures(X_i) and the phase quadratures(Y_i) of the four modes b_i satisfy the following inequalities, the four modes are in the quadripartite entangled cluster state with the full inseparability[16]. The criterion inequalities for the full inseparability of the CV quadripartite cluster state are

$$\begin{aligned} \left\langle \delta^2 \left(X_{b1} + X_{b2} + X_{b3} \right) \right\rangle + \left\langle \delta^2 \left(Y_{b1} - Y_{b2} \right) \right\rangle < 1, \\ \left\langle \delta^2 \left(X_{b3} - X_{b4} \right) \right\rangle + \left\langle \delta^2 \left(-Y_{b2} + Y_{b3} + Y_{b4} \right) \right\rangle < 1, \end{aligned} \quad (1)$$

$$\left\langle \delta^2 (X_{b_1} + X_{b_2} + X_{b_3}) \right\rangle + \left\langle \delta^2 (-Y_{b_2} + Y_{b_3} + Y_{b_4}) \right\rangle < 1.$$

If the left-hand sides of these inequalities are smaller than the normalized shot noise limit at the right-hand sides, the four optical modes are in a fully inseparable quantum state.

3 Single-mode evolutions: Phase-space displacement operation

In CV regime, the Pauli \hat{X} and \hat{Z} operators are generalized to the Weyl-Heisenberg group, which is a Lie group with generators \hat{q} and \hat{p} . The operators satisfy the canonical commutation relation $[\hat{q}, \hat{p}] = i$ (with $\hbar = 1$). Then the σ_x and σ_z are generalized to the finite phase-space translation operators, $\hat{X}(s) = e^{-is\hat{p}}$ and $\hat{Z}(s) = e^{-is\hat{q}}$ [11, 17]. As discussed in Ref. [11], the $\hat{Z}(s) = e^{-is\hat{q}}$ gate is implemented by measuring \hat{p} and subtracting s from the result, where s is the desired displacement.

The experimental setup to realize the phase-space displacement operation is shown in Fig.2. Using the prepared quadripartite cluster states, we can choose arbitrarily two submodes, b_1 and b_4 for example, to be the input and output mode, respectively.

The input state a_{in} of the logical gate is combined with the mode b_1 at a 50:50 beam splitter with the phase difference of 0. In Heisenberg picture, the input state is expressed as $a_{in} = X_{in} + iY_{in}$, X_{in} and Y_{in} are the amplitude and phase quadrature of a_{in} respectively. When $\langle X_{in} \rangle = x$ and $\langle \delta^2 X_{in} \rangle = 0$, a_{in} is the eigenstate of position $|x\rangle$. For finite squeezing, $\langle \delta^2 X_{in} \rangle = \Omega$, a_{in} is a Gaussian wave packet in the phase space whose mean value is x . The modes c_1 and c_2 with the amplitude

quadratures X_{c_1} , X_{c_2} and the phase quadratures Y_{c_1} , Y_{c_2} are two output modes from a 50% beamsplitter, on which mode a_{in} and mode b_1 are coupled with the phase difference of zero.

The amplitude quadratures (X_j) and the phase quadratures (Y_j) ($j = c_1, c_2, b_2, b_3, b_4$) of modes c_1 , c_2 , b_2 , b_3 and b_4 are expressed by

$$\begin{aligned}
X_{c_1} &= \left(\frac{1}{\sqrt{5}} X_{a_2} - \frac{1}{2\sqrt{5}} Y_{a_3} + \frac{1}{2} X_{a_1} \right) + \frac{1}{\sqrt{2}} X_{in}, \\
Y_{c_1} &= \left(\frac{1}{\sqrt{5}} Y_{a_2} + \frac{1}{2\sqrt{5}} X_{a_3} + \frac{1}{2} Y_{a_1} \right) + \frac{1}{\sqrt{2}} Y_{in}, \\
X_{c_2} &= \left(\frac{1}{\sqrt{5}} X_{a_2} - \frac{1}{2\sqrt{5}} Y_{a_3} + \frac{1}{2} X_{a_1} \right) - \frac{1}{\sqrt{2}} X_{in}, \\
Y_{c_2} &= \left(\frac{1}{\sqrt{5}} Y_{a_2} + \frac{1}{2\sqrt{5}} X_{a_3} + \frac{1}{2} Y_{a_1} \right) - \frac{1}{\sqrt{2}} Y_{in}, \\
X_{b_2} &= \frac{2}{\sqrt{10}} X_{a_2} - \frac{1}{\sqrt{10}} Y_{a_3} - \frac{1}{\sqrt{2}} X_{a_1}, & Y_{b_2} &= \frac{2}{\sqrt{10}} Y_{a_2} + \frac{1}{\sqrt{10}} X_{a_3} - \frac{1}{\sqrt{2}} Y_{a_1}, \\
X_{b_3} &= \frac{1}{\sqrt{10}} X_{a_2} + \frac{2}{\sqrt{10}} Y_{a_3} - \frac{1}{\sqrt{2}} Y_{a_4}, & Y_{b_3} &= \frac{1}{\sqrt{10}} Y_{a_2} - \frac{2}{\sqrt{10}} X_{a_3} + \frac{1}{\sqrt{2}} X_{a_4}, \\
X_{b_4} &= \frac{1}{\sqrt{10}} X_{a_2} + \frac{2}{\sqrt{10}} Y_{a_3} + \frac{1}{\sqrt{2}} Y_{a_4}, & Y_{b_4} &= \frac{1}{\sqrt{10}} Y_{a_2} - \frac{2}{\sqrt{10}} X_{a_3} - \frac{1}{\sqrt{2}} X_{a_4}.
\end{aligned} \tag{2}$$

Where X_{a_i} and Y_{a_i} ($i = 1, 2, 3, 4$) are the amplitude and the phase quadratures of the initial squeezed states a_i^s . At first, the amplitude and phase quadratures X_{c_1} , Y_{c_2} , X_{b_2} and Y_{b_3} are measured by the homodyne detectors HD_o ($o = 1, 2, 3, 4$) respectively. The photocurrent of X_{c_1} (Y_{c_2}) measured by HD₁ (HD₂) is displaced an amount s_0 (s_1), which corresponding the desired displaced amount $s = \sqrt{2}s_0$ ($\sqrt{2}s_1$). The sum of the photocurrent of the displaced X_{c_1} (Y_{c_2}) and the photocurrent of

$X_{b_2}(Y_{b_3})$ measured by HD₃(HD₄) is used to modulate the mode b_4 via an amplitude (phase) modulator AM (PM). The modulated mode b_4 is the resultant output mode a^{out} , the amplitude and phase quadratures of which are expressed by

$$\begin{aligned}
X^{out} &= X_{b_4} + g_0(X_{c_1} + s_0) + g_2 X_{b_2} \\
&= \left(\frac{1}{\sqrt{10}} X_{a_2} + \frac{2}{\sqrt{10}} Y_{a_3} + \frac{1}{\sqrt{2}} Y_{a_4}\right) + g_0 \times \left[\left(\frac{1}{\sqrt{5}} X_{a_2} - \frac{1}{2\sqrt{5}} Y_{a_3} + \frac{1}{2} X_{a_1}\right) + \frac{1}{\sqrt{2}} X_{in} + s_0\right] \\
&\quad + g_2 \times \left(\frac{2}{\sqrt{10}} X_{a_2} - \frac{1}{\sqrt{10}} Y_{a_3} - \frac{1}{\sqrt{2}} X_{a_1}\right) \tag{3} \\
&= \left(\frac{1}{\sqrt{10}} + \frac{g_0}{\sqrt{5}} + \frac{2g_2}{\sqrt{10}}\right) X_{a_2} + \left(\frac{2}{\sqrt{10}} - \frac{g_0}{2\sqrt{5}} - \frac{g_2}{\sqrt{10}}\right) Y_{a_3} + \frac{1}{\sqrt{2}} Y_{a_4} + \left(\frac{g_0}{2} - \frac{g_2}{\sqrt{2}}\right) X_{a_1} \\
&\quad + \frac{g_0}{\sqrt{2}} X_{in} + g_0 s_0,
\end{aligned}$$

$$\begin{aligned}
Y^{out} &= Y_{b_4} + g_1(Y_{c_2} - s_1) + g_3 Y_{b_3} \\
&= \left(\frac{1}{\sqrt{10}} Y_{a_2} - \frac{2}{\sqrt{10}} X_{a_3} - \frac{1}{\sqrt{2}} X_{a_4}\right) + g_1 \times \left[\left(\frac{1}{\sqrt{5}} Y_{a_2} + \frac{1}{2\sqrt{5}} X_{a_3} + \frac{1}{2} Y_{a_1}\right) - \frac{1}{\sqrt{2}} Y_{in} - s_1\right] \\
&\quad + g_3 \times \left(\frac{1}{\sqrt{10}} Y_{a_2} - \frac{2}{\sqrt{10}} X_{a_3} + \frac{1}{\sqrt{2}} X_{a_4}\right) \tag{4} \\
&= \left(\frac{1}{\sqrt{10}} + \frac{g_1}{\sqrt{5}} + \frac{g_3}{\sqrt{10}}\right) Y_{a_2} - \left(\frac{2}{\sqrt{10}} - \frac{g_1}{2\sqrt{5}} + \frac{2g_3}{\sqrt{10}}\right) X_{a_3} + \frac{g_1}{2} Y_{a_1} + \left(-\frac{1}{\sqrt{2}} + \frac{g_3}{\sqrt{2}}\right) X_{a_4} \\
&\quad - \frac{g_1}{\sqrt{2}} Y_{in} - g_1 s_0.
\end{aligned}$$

The quadrature amplitudes (X_{ai}) and phases (Y_{ai}) of the four squeezed modes

a_i^s ($i=1,2,3,4$) equal to [18-20]

$$\begin{aligned}
X_{a1(4)} &= e^{+r} X_{a1(4)}^{(0)}, & Y_{a1(4)} &= e^{-r} Y_{a1(4)}^{(0)}, \tag{5} \\
X_{a2(3)} &= e^{-r} X_{a2(3)}^{(0)}, & Y_{a2(3)} &= e^{+r} Y_{a2(3)}^{(0)},
\end{aligned}$$

where, r is the squeezing parameter, and have been assumed identical for the four squeezed state. $X_{ai}^{(0)}$ and $Y_{ai}^{(0)}$ stand for the amplitude and the phase quadratures of the injected vacuum states, and the shot noise of them is normalized to 1.

g_i ($i = 0, 1, 2, 3$) are the gain factors of the corresponding photocurrents and we take $g_0 = \sqrt{2}$, $g_1 = -\sqrt{2}$ to ensure the coefficient of $\langle X_{in} \rangle$ and $\langle Y_{in} \rangle$ in the output mode are 1. Substituting g_0, g_1 and Eq.(5) into Eqs.(3) and (4), we obtain

$$X^{out} = \left(\frac{3}{\sqrt{10}} + \frac{2g_2}{\sqrt{10}}\right)X_{a2} + \left(\frac{1}{\sqrt{10}} - \frac{g_2}{\sqrt{10}}\right)Y_{a3} + \frac{1}{\sqrt{2}}Y_{a4} + \left(\frac{1}{\sqrt{2}} - \frac{g_2}{\sqrt{2}}\right)X_{a1} + X_{in} + \sqrt{2}s_0, \quad (6)$$

$$Y^{out} = \left(-\frac{1}{\sqrt{10}} + \frac{g_3}{\sqrt{10}}\right)Y_{a2} - \left(\frac{3}{\sqrt{10}} + \frac{2g_3}{\sqrt{10}}\right)X_{a3} - \frac{1}{\sqrt{2}}Y_{a1} + \left(-\frac{1}{\sqrt{2}} + \frac{g_3}{\sqrt{2}}\right)X_{a4} + Y_{in} + \sqrt{2}s_1. \quad (7)$$

The calculated fluctuation variances σ_x^2 and σ_y^2 of X^{out} and Y^{out} are

$$\sigma_x^2 = \left(\frac{3}{\sqrt{10}} + \frac{2g_2}{\sqrt{10}}\right)^2 e^{-2r} + \left(\frac{1}{\sqrt{10}} - \frac{g_2}{\sqrt{10}}\right)^2 e^{2r} + \frac{1}{2} e^{-2r} + \left(\frac{1}{\sqrt{2}} - \frac{g_2}{\sqrt{2}}\right)^2 e^{2r} + V(X_{in}), \quad (8)$$

$$\sigma_y^2 = \left(-\frac{1}{\sqrt{10}} + \frac{g_3}{\sqrt{10}}\right)^2 e^{2r} + \left(\frac{3}{\sqrt{10}} + \frac{2g_3}{\sqrt{10}}\right)^2 e^{-2r} + \frac{1}{2} e^{-2r} + \left(-\frac{1}{\sqrt{2}} + \frac{g_3}{\sqrt{2}}\right)^2 e^{2r} + V(Y_{in}). \quad (9)$$

Calculating the minimum values of σ_x and σ_y in terms of g_2 and g_3 , we obtain the optimum gain factors

$$g_2^{opt} = g_3^{opt} = \frac{3(e^{2r} - e^{-2r})}{2e^{-2r} + 3e^{2r}}. \quad (10)$$

The minimum variance equals

$$\sigma_{x,\min}^2 = \frac{e^{-2r} + 9e^{2r}}{2 + 3e^{4r}} + V(X_{in}), \quad (11)$$

$$\sigma_{y,\min}^2 = \frac{e^{-2r} + 9e^{2r}}{2 + 3e^{4r}} + V(Y_{in}). \quad (12)$$

From Eqs.(6) and (7), we can easily prove

$$\langle X^{out} \rangle = \langle X_{in} \rangle + \sqrt{2}s_0, \quad \langle Y^{out} \rangle = \langle Y_{in} \rangle + \sqrt{2}s_1. \quad (13)$$

Obviously, the average values of the amplitude and the phase quadratures of the input state have been displaced in the phase-space a desired amount $s = \sqrt{2}s_0$ and $s = \sqrt{2}s_1$, respectively.

According to the Rayleigh criterion in optics, when the center of the Airy disk for the first object occurs at the first minimum of the Airy disk of the second one, we say that the two objects can be barely resolved [21]. For a Gaussian wavepacket, it can be calculated based on the Rayleigh criterion that if taking $\delta x(\delta y) = 2\sigma_x$ and $\delta x(\delta y) = 3\sigma_x$, to be the radius of Airy disk (the first minimum), the resolving precision will reach 95% and 99%, respectively[21].

Thus we consider when

$$\sqrt{2}s_0 > 3\sigma_x = 3 \times \left[\frac{e^{-2r} + 9e^{2r}}{2 + 3e^{4r}} + V(X_{in}) \right]^{\frac{1}{2}}, \quad (14)$$

$$\sqrt{2}s_1 > 3\sigma_y = 3 \times \left[\frac{e^{-2r} + 9e^{2r}}{2 + 3e^{4r}} + V(Y_{in}) \right]^{\frac{1}{2}}, \quad (15)$$

the displacement in x and y direction can be distinguished. Thus, we define

$\frac{3}{\sqrt{2}}\sigma_x$ and $\frac{3}{\sqrt{2}}\sigma_y$ to be the minimum of the displacement limited by the quantum

noises in optical modes for a given r and noises of the input state $[V(X_{in})$ and

$V(Y_{in})]$. Only when the displacement $s_0(s_1) = s/\sqrt{2}$ is larger than the minimum, the

displacement in the phase-space is distinguishable. The minimum distinguishable

displacement $s_0^{\min}(s_1^{\min})$ stands for the reachable precision of a logical operation

system.

For a general example, we assume that the input state is a squeezed state with a

squeezing parameter of r' ($r' = 0$ corresponds to a coherent state). The dependences

of the distinguishable displacements of the amplitude quadrature (s_0) and the phase

quadrature (s_1) upon r and r' are shown in Fig.3. We can see that when r and

r' increase, s_0^{\min} and s_1^{\min} decrease, however the influence of r is larger than that

of r' . It means that for performing a precise phase-space displacement operation on

an input quantum state, we have to prepare a cluster state with high squeezing parameter at first.

When $s_0 = 0$ and $s_1 = 0$, the system performs an operation corresponding to an identity gate, in which the information propagates down a quantum wire to complete a simplest single-mode evolution. In fact, to propagate the information down a quantum wire, the basic method is teleportation [22-24]. Just like that in one-way DV QC scheme, a combination of successive one-qubit teleportation plays a key role [25, 26], CV teleportation is also the elementary method for performing CV quantum computation with cluster states. The identity operation is equivalent to the teleportation of the input state a_{in} to the output state a_{out} under the help of cluster entanglement. The flexibility of the system is that we can also extract the output state either from b_2 or b_3 instead of from b_4 .

If using the unity gain ($g = 1$), the fidelity for the input Gaussian states is simply given by $F = \frac{2}{\sqrt{(1 + \sigma_x^2)(1 + \sigma_y^2)}}$ [23]. Substituting Eq.(11) and (12) into the fidelity formula, the dependence of F on the squeezing parameter r in the system is shown in Fig. 4.

For perfectly initial squeezing of $r \rightarrow \infty$, the fidelity $F \rightarrow 1$, it means that in the ideal case the quantum information is successfully propagated down the quantum wire. Generally, for the classical case without squeezing ($r \rightarrow 0$), the best fidelity F should equal 0.5[23], which just is the result in Fig.4.

4 Single-mode squeezing operation

A single-mode squeezer is an important primitive for performing Gaussian transformation. As pointed out in Ref.[11,12], in a squeezer there is the operator of

quadratic form, $D = \exp(it\hat{q}^2)$, which can be performed via a given cluster state solely by doing suitable homodyne measurements, where t stands for the squeezing parameter of the $D = \exp(it\hat{q}^2)$ operation. The experimental setup of the single-mode squeezer is the same as Fig.2. However in the squeezing operation, a linear combination of position and momentum should be detected with the homodyne detections (HDs), which correspond to the measurement of rotated quadratures[12].

Coupling the input state a_{in} to a submode b_1 of the quadripartite cluster state, and adjusting the phase differences between the local oscillator and the signal field in HD₁, HD₂, HD₃ and HD₄ to θ , $\pi/2$, 0 and $\pi/2$ for measuring $Y_{c1} \sin \theta + X_{c1} \cos \theta$, Y_{c2} , X_{b2} , and Y_{b3} , respectively. Then, those measured photocurrents are used for displacing the amplitude and the phase quadratures of the mode b_4 . The quadratures of the output mode are expressed by

$$\begin{aligned}
X^{out} &= X_{b4} + \sqrt{2} \frac{1}{\cos \theta} (\cos \theta X_{c1} + \sin \theta Y_{c1}) + X_{b2} - \sqrt{2} \tan \theta Y_{c2} \\
&= \left(\frac{1}{\sqrt{10}} X_{a2} + \frac{2}{\sqrt{10}} Y_{a3} + \frac{1}{\sqrt{2}} Y_{a4} \right) + \sqrt{2} \times \left\{ \left[\left(\frac{1}{\sqrt{5}} X_{a2} - \frac{1}{2\sqrt{5}} Y_{a3} + \frac{1}{2} X_{a1} \right) + \frac{X_{in}}{\sqrt{2}} \right] \right. \\
&\quad \left. + \tan \theta \left[\left(\frac{1}{\sqrt{5}} Y_{a2} + \frac{1}{2\sqrt{5}} X_{a3} + \frac{1}{2} Y_{a1} \right) + \frac{1}{\sqrt{2}} Y_{in} \right] \right\} + \left(\frac{2}{\sqrt{10}} X_{a2} - \frac{1}{\sqrt{10}} Y_{a3} - \frac{1}{\sqrt{2}} X_{a1} \right) \quad (16) \\
&\quad - \sqrt{2} \tan \theta \left[\left(\frac{1}{\sqrt{5}} Y_{a2} + \frac{1}{2\sqrt{5}} X_{a3} + \frac{1}{2} Y_{a1} \right) - \frac{1}{\sqrt{2}} Y_{in} \right] \\
&= \sqrt{\frac{5}{2}} X_{a2} + \frac{1}{\sqrt{2}} Y_{a4} + X_{in} + 2 \tan \theta Y_{in},
\end{aligned}$$

$$\begin{aligned}
Y^{out} &= Y_{b4} - \sqrt{2} \times Y_{c2} + Y_{b3} \\
&= \left(\frac{1}{\sqrt{10}} Y_{a2} - \frac{2}{\sqrt{10}} X_{a3} - \frac{1}{\sqrt{2}} X_{a4} \right) - \sqrt{2} \times \left[\left(\frac{1}{\sqrt{5}} Y_{a2} + \frac{1}{2\sqrt{5}} X_{a3} + \frac{1}{2} Y_{a1} \right) - \frac{1}{\sqrt{2}} Y_{in} \right] \\
&\quad + \left(\frac{1}{\sqrt{10}} Y_{a2} - \frac{2}{\sqrt{10}} X_{a3} + \frac{1}{\sqrt{2}} X_{a4} \right) \\
&= -\sqrt{\frac{5}{2}} X_{a3} - \frac{1}{\sqrt{2}} Y_{a1} + Y_{in}.
\end{aligned} \tag{17}$$

In the equation (16), the rescaling factor is $\cos \theta$, and the squeezing parameter $t = -\tan \theta$. For experiments, the squeezing of the output mode a^{out} can be checked with an other homodyne detection HD₅. If the phase difference between the LO and a_{out} in HD₅ is ϕ , we have

$$\begin{aligned}
&Y^{out} \sin \phi + X^{out} \cos \phi \\
&= \left[-\sqrt{\frac{5}{2}} X_{a3} - \frac{1}{\sqrt{2}} Y_{a1} + Y_{in} \right] \sin \phi + \left[\sqrt{\frac{5}{2}} X_{a2} + \frac{1}{\sqrt{2}} Y_{a4} + X_{in} - 2 \tan \theta Y_{in} \right] \cos \phi \\
&= \left[-\sqrt{\frac{5}{2}} X_{a3} - \frac{1}{\sqrt{2}} Y_{a1} \right] \sin \phi + \left[\sqrt{\frac{5}{2}} X_{a2} + \frac{1}{\sqrt{2}} Y_{a4} \right] \cos \phi \\
&\quad + \cos \phi X_{in} + (2 \tan \theta \cos \phi + \sin \phi) Y_{in},
\end{aligned} \tag{18}$$

$$V(Y^{out} \sin \phi + X^{out} \cos \phi) = 3e^{-2r} + \cos^2 \phi + (2 \tan \theta \cos \phi + \sin \phi)^2. \tag{19}$$

From Eq.(19), we can see that the fluctuation variances may be smaller than the normalized shot noise limit (SNL) for appropriate θ and ϕ . The dependences of the variances V in Eq.(19) on the detection phase ϕ of the output mode are drawn for different θ and a given $r = 2$ in Fig.5. Obviously, the noise ellipse of the output squeezed mode becomes more narrow and the lowest variance becomes smaller(squeezing increases) when θ increases, which corresponds to the result in Ref.[11]. However, if $\tan \theta = 0$, we have $V(Y^{out} \sin \phi + X^{out} \cos \phi) = 3e^{-2r} + 1$. In this case the variance V does not depend on ϕ , thus there is no squeezing to be

generated whatever cluster is applied. In Fig.6 the functions of V vs ϕ for different r of the initial cluster state and a given $\tan \theta = 2$ are presented. It is pointed out that only when r of the cluster state must be larger than a threshold ($r = 0.55$ in this example) squeezing of the output mode exists, i.e. V is lower than the normalized SNL. Where $r = 0.6$ and $r = 1.15$ correspond to the squeezing of 5.2 dB and 10 dB respectively, which have been experimentally realized [27-29, 30], the maximum squeezing direction ϕ depends on θ only and does not on r . The dependence of ϕ^{opt} for the minimum V_{min} on θ is expressed in Eq.(20):

$$\tan 2\phi^{opt} = (\tan \theta)^{-1} \quad (20)$$

The minimum V_{min} for a given r equals:

$$V(Y^{out} \cos \phi^{opt} + X^{out} \sin \phi^{opt}) = 3e^{-2r} + (\tan \phi^{opt})^{-2} \quad (21)$$

5 CNOT operation

After the pauli \hat{X} and \hat{Z} operators are generalized to the finite phase-space translation operators, the controlled logical operation CNOT and CPHASE are naturally generalized to controlled- \hat{X} (\hat{C}_X) and controlled- \hat{Z} (\hat{C}_Z), respectively, which effect a phase-space displacement on the target by an amount determined by the position eigenvalue of the control state: $\hat{C}_X = \exp(-i\hat{q} \otimes \hat{p})$ and $\hat{C}_Z = \exp(-i\hat{q} \otimes \hat{q})$, where the order of the system is (control \otimes target)[11]. In this section, we will discuss the realization of CNOT operation.

Fig.7 is the proposed experimental scheme for realizing CV CNOT operation using linear quadripartite Cluster state. We use the modulated coherent states to be the control signal a_c and the target signal a_t , that is

$$a_c = (X_c + s_c) + iY_c, \quad (22)$$

$$a_t = (X_t + s_t) + iY_t. \quad (23)$$

Where $X_{c(t)}$ and $Y_{c(t)}$ are the amplitude and the phase quadrature of $a_{c(t)}$, s_c and s_t are the added modulation signals on the control and the target signals respectively.

The input control signal a_c and the target signal a_t are coupled respectively to the submodes b_3 and b_2 of the cluster state at a 50:50 beam splitter with the phase difference of 0. The quadratures of the coupled state equal to

$$\begin{aligned} X_{b1} &= \frac{2}{\sqrt{10}} X_{a2} - \frac{1}{\sqrt{10}} Y_{a3} + \frac{1}{\sqrt{2}} X_{a1}, & Y_{b1} &= \frac{2}{\sqrt{10}} Y_{a2} + \frac{1}{\sqrt{10}} X_{a3} + \frac{1}{\sqrt{2}} Y_{a1}, \\ X_{t1} &= \frac{1}{\sqrt{2}} \left(\frac{2}{\sqrt{10}} X_{a2} - \frac{1}{\sqrt{10}} Y_{a3} - \frac{1}{\sqrt{2}} X_{a1} + X_t + s_t \right), \\ Y_{t1} &= \frac{1}{\sqrt{2}} \left(\frac{2}{\sqrt{10}} Y_{a2} + \frac{1}{\sqrt{10}} X_{a3} - \frac{1}{\sqrt{2}} Y_{a1} + Y_t \right), \\ X_{t2} &= \frac{1}{\sqrt{2}} \left(\frac{2}{\sqrt{10}} X_{a2} - \frac{1}{\sqrt{10}} Y_{a3} - \frac{1}{\sqrt{2}} X_{a1} - X_t - s_t \right), \\ Y_{t2} &= \frac{1}{\sqrt{2}} \left(\frac{2}{\sqrt{10}} Y_{a2} + \frac{1}{\sqrt{10}} X_{a3} - \frac{1}{\sqrt{2}} Y_{a1} - Y_t \right), \\ X_{c1} &= \frac{1}{\sqrt{2}} \left(\frac{1}{\sqrt{10}} X_{a2} + \frac{2}{\sqrt{10}} Y_{a3} - \frac{1}{\sqrt{2}} Y_{a4} - X_c - s_c \right), & (24) \\ Y_{c1} &= \frac{1}{\sqrt{2}} \left(\frac{1}{\sqrt{10}} Y_{a2} - \frac{2}{\sqrt{10}} X_{a3} + \frac{1}{\sqrt{2}} X_{a4} - Y_c \right), \\ X_{c2} &= \frac{1}{\sqrt{2}} \left(\frac{1}{\sqrt{10}} X_{a2} + \frac{2}{\sqrt{10}} Y_{a3} - \frac{1}{\sqrt{2}} Y_{a4} + X_c + s_c \right), \\ Y_{c2} &= \frac{1}{\sqrt{2}} \left(\frac{1}{\sqrt{10}} Y_{a2} - \frac{2}{\sqrt{10}} X_{a3} + \frac{1}{\sqrt{2}} X_{a4} + Y_c \right), \\ X_{b4} &= \frac{1}{\sqrt{10}} X_{a2} + \frac{2}{\sqrt{10}} Y_{a3} + \frac{1}{\sqrt{2}} Y_{a4}, & Y_{b4} &= \frac{1}{\sqrt{10}} Y_{a2} - \frac{2}{\sqrt{10}} X_{a3} - \frac{1}{\sqrt{2}} X_{a4}. \end{aligned}$$

Measuring X_{t1} , Y_{t2} , X_{c1} , Y_{c2} , and feeding forward the measured photocurrents

to mode b_1 and b_4 respectively, the quadratures of the output mode become

$$\begin{aligned}
X_t^{out} &= X_{b1} + \sqrt{2}X_{t1} + \sqrt{2}X_{c1} \\
&= \left(\frac{2}{\sqrt{10}}X_{a2} - \frac{1}{\sqrt{10}}Y_{a3} + \frac{1}{\sqrt{2}}X_{a1}\right) + \sqrt{2} \times \frac{1}{\sqrt{2}} \left(\frac{2}{\sqrt{10}}X_{a2} - \frac{1}{\sqrt{10}}Y_{a3} - \frac{1}{\sqrt{2}}X_{a1} + X_t + s_t\right) \\
&\quad + \sqrt{2} \times \frac{1}{\sqrt{2}} \left(\frac{1}{\sqrt{10}}X_{a2} + \frac{2}{\sqrt{10}}Y_{a3} - \frac{1}{\sqrt{2}}Y_{a4} - X_c - s_c\right) \\
&= \sqrt{\frac{5}{2}}X_{a2} - \sqrt{\frac{1}{2}}Y_{a4} + X_t + s_t - X_c - s_c,
\end{aligned}$$

$$\begin{aligned}
Y_c^{out} &= Y_{b1} - \sqrt{2}Y_{t2} \\
&= \frac{2}{\sqrt{10}}Y_{a2} + \frac{1}{\sqrt{10}}X_{a3} + \frac{1}{\sqrt{2}}Y_{a1} - \sqrt{2} \times \frac{1}{\sqrt{2}} \left(\frac{2}{\sqrt{10}}Y_{a2} + \frac{1}{\sqrt{10}}X_{a3} - \frac{1}{\sqrt{2}}Y_{a1} - Y_t\right) \quad (25) \\
&= \sqrt{2}Y_{a1} + Y_t,
\end{aligned}$$

$$\begin{aligned}
X_c^{out} &= X_{b4} - \sqrt{2}X_{c1} \\
&= \left(\frac{1}{\sqrt{10}}X_{a2} + \frac{2}{\sqrt{10}}Y_{a3} + \frac{1}{\sqrt{2}}Y_{a4}\right) - \sqrt{2} \times \frac{1}{\sqrt{2}} \left(\frac{1}{\sqrt{10}}X_{a2} + \frac{2}{\sqrt{10}}Y_{a3} - \frac{1}{\sqrt{2}}Y_{a4} - X_c - s_c\right) \\
&= \sqrt{2}Y_{a4} + X_c + s_c,
\end{aligned}$$

$$\begin{aligned}
Y_t^{out} &= Y_{b4} - \sqrt{2}Y_{t2} + \sqrt{2}Y_{c2} \\
&= \frac{1}{\sqrt{10}}Y_{a2} - \frac{2}{\sqrt{10}}X_{a3} - \frac{1}{\sqrt{2}}X_{a4} - \sqrt{2} \times \frac{1}{\sqrt{2}} \left(\frac{2}{\sqrt{10}}Y_{a2} + \frac{1}{\sqrt{10}}X_{a3} - \frac{1}{\sqrt{2}}Y_{a1} - Y_t\right) \\
&\quad + \sqrt{2} \times \frac{1}{\sqrt{2}} \left(\frac{1}{\sqrt{10}}Y_{a2} - \frac{2}{\sqrt{10}}X_{a3} + \frac{1}{\sqrt{2}}X_{a4} + Y_c\right) \quad (26) \\
&= -\sqrt{\frac{5}{2}}X_{a3} + \sqrt{\frac{1}{2}}Y_{a1} + Y_t + Y_c.
\end{aligned}$$

The average values and the variances of the amplitude and the phase quadratures for the input and the output states are listed in table 1. We can see, the phase quadrature of the output target signal have been displaced under the control of the control signal s_c . It means that the CNOT operation has been implemented.

Table 1 The average values and the variances of the amplitude and the phase quadratures for the input and the output states

	Control	Target
Input signal	$\langle X_c \rangle = s_c$ $\sigma_x = V(X_c)$ $\langle Y_c \rangle = 0$ $\sigma_y = V(Y_c)$	$\langle X_t \rangle = s_t$ $\sigma_x = V(X_t)$ $\langle Y_t \rangle = 0$ $\sigma_y = V(Y_t)$
Output signal	$\langle X_c^{out} \rangle = s_c$ $\langle Y_c^{out} \rangle = 0$ $\sigma_x = 2e^{-2r} + V(X_c) \xrightarrow{r \rightarrow \infty} V(X_c)$ $\sigma_y = 3e^{-2r} + [V(Y_c) + V(Y_t)]$ $\xrightarrow{r \rightarrow \infty} [V(Y_c) + V(Y_t)]$	$\langle X_t^{out} \rangle = s_t - s_c$ $\langle Y_t^{out} \rangle = 0$ $\sigma_x = 3e^{-2r} + V(X_c) + V(X_t)$ $\xrightarrow{r \rightarrow \infty} V(X_c) + V(X_t)$ $\sigma_x = 2e^{-2r} + V(Y_t) \xrightarrow{r \rightarrow \infty} V(Y_t)$

The Wigner functions of the input(output) control and target signals are shown in Fig.8, where we have assumed that both input control and target signals are the amplitude-squeezed states of light and $s_c = 1$ and $s_t = 2$ (normalized to the shot noise limit). Obviously, the amplitude quadratures are displaced an amount along the direction of x axis under the action of the control signal (from 2 to 1). Since the finite squeezing of the cluster state, some noises are added in the process, and thus the Wigner functions of the output states are expanded at the direction of x axis. The influence of the noises will reduce when r increases (comparing $r = 1$ and $r = 3$).

6 Conclusions

For conclusion, following the theoretical suggestions on CV QC in Ref.[11] and [12], we designed the concrete experimental systems for implementing the phase-space displacement transformation, squeezing and CNOT operation based on the quadripartite cluster state of electromagnetic field. In the proposed schemes only linear optics, homodyne detections and classical feedforwards are required and the cluster state can be prepared off-line. The influences of finite squeezing of cluster state on the precisions of the logical operations are analyzed. Although a nonlinear

element such as any single-mode non-Gaussian measurement is needed for demonstrating universal CV QC, the realization of the proposed logical operations is the first step for universal quantum computation. The calculations and discussions in this paper provide direct references for the design of the experimental systems implementing CV logical gates. The CV quadripartite cluster states have been experimentally obtained [13,14], thus the proposed schemes for the CV logical operations are accessible with the present experimental technology.

This research was supported by Natural Science Foundation of China (Grants No. 60736040 and 10674088), National Basic Research Program of China(Grant No.2006CB921101), the PCSIRT (Grant No. IRT0516).

* Corresponding author's Email address: changde@sxu.edu.cn

- [1] “Quantum Information with Continuous Variables”, Edited by Samuel L. Braunstein and Arun K. Pati, Kluwer Academic Publishers (2003)
- [2] “The Physics of Quantum Information”, Edited by Dirk Bouwmeester, Anton Zeilinger and Artur Ekert, Springer(2000)
- [3] M. A. Nielsen. *Rep. Math. Phys.* 57, 147(2006)
- [4] R.Raussendorf and H.J.Briegel, *Phys.Rev.Lett.*86,5188(2001)
- [5] R.Raussendorf, D. E. Browne, and H. J. Briegel. *Phys. Rev. A.* 68, 022312(2003)
- [6] P. Walther, K. J. Resch, T. Rudolph, E. Schenck, H. Weinfurter, V. Vedral, M. Aspelmeyer, and A. Zeilinger, *Nature* 434,169(2005)
- [7] R. Prevedel, P. Walther, F. Tiefenbacher, P. Bohi, R. Kaltenbaek, T. Jennewein, and A. Zeilinger, *Nature* 445, 65(2007)
- [8] K. Chen, C. Li, Q. Zhang, Y. Chen, A. Goebel, S. Chen, A. Mair, and J.-W. Pan, *Phys. Rev. Lett.* 99, 120503(2007)
- [9] S.Lloyd and S.L.Braunstein, *Phys.Rev.Lett.*82,1784(1999)
- [10] J.Zhang and S.L.Braunstein, *Phys. Rev.A,* 73,032318(2006)
- [11] N.C.Menicucci, P. van Loock, M.Gu, C. Weedbrook, T. C. Ralph, and M. A. Nielsen, *Phys. Rev. Lett.* 97, 110501(2006)
- [12] Peter van Loock, *J. Opt. Soc. Am. B,* 24, 340(2007)
- [13] X. Su, A. Tan, X. Jia, J. Zhang, C. Xie, and K. Peng, *Phys. Rev.Lett.* 98, 070502 (2007)
- [14] M. Yukawa, R. Ukai, P. van. Loock, and A. Furusawa, *Phys. Rev. A* 78, 012301(2008)
- [15] Y. Zhang, H. Wang, X. Li, J. Jing, C. Xie, and K. Peng, *Phys. Rev. A* 62, 023813(2000)
- [16] P. van Loock and A. Furusawa, *Phys. Rev. A* 67, 052315(2003)
- [17] S. D. Bartlett, B. C. Sanders, S. L. Braunstein, and K. Nemoto, *Phys. Rev. Lett.* 88, 097904(2002)
- [18] M. D. Reid, and P. D. Drammond, *Phys. Rev. Lett.* 60, 2731(1988)
- [19] M. D. Reid, *Phys. Rev. A* 40, 913(1989)
- [20] Y. Yang, H. Su, C. Xie, K. Peng, *Phys. Lett. A* 259, 171(1999)

- [21] “Principles of Optics”, Max Born and Emil Wolf, Pergamon Press Ltd, London(1959)
- [22] D. Bouwmeester, J.-W. Pan, K. Mattle, M. Eibl, H. Weinfurter, and A. Zeilinger, Nature(London), 390, 575(1997)
- [23] A. Furusawa, J. L. Sorensen, S. L. Braunstein, C. A. Fuchs, H. J. Kimble, E. S. Polzik, Science 282, 706(1998)
- [24] C. Xie, J. Zhang, Q. Pan, X. Jia, K. Peng, Frontiers of Physics in China 4, 383(2006)
- [25] M. A. Nielsen, Rep. Math. Phys. 57, 147(2006)
- [26] X. Zhou, D. W. Leung, and I. L. Chuang, Phys. Rev. A 62, 052316(2000)
- [27] X. Li, Q. Pan, J. Jing, J. Zhang, C. Xie, and K. Peng, Phys. Rev. Lett. **88**, 047904 (2002)
- [28] J. Jing, J. Zhang, Y. Yan, F. Zhao, C. Xie, and K. Peng, Phys. Rev. Lett. **90**, 167903 (2003)
- [29] X. Jia, X. Su, Q. Pan, J. Gao, C. Xie, and K. Peng, Phys. Rev. Lett. **93**, 250503 (2004)
- [30] H. Vahlbruch, M. Mehmet, S. Chelkowski, B. Hage, A. Franzen, N. Lastzka, S. Goßler, K. Danzmann, and R. Schnabel, Phys. Rev. Lett. 100, 033602 (2008)

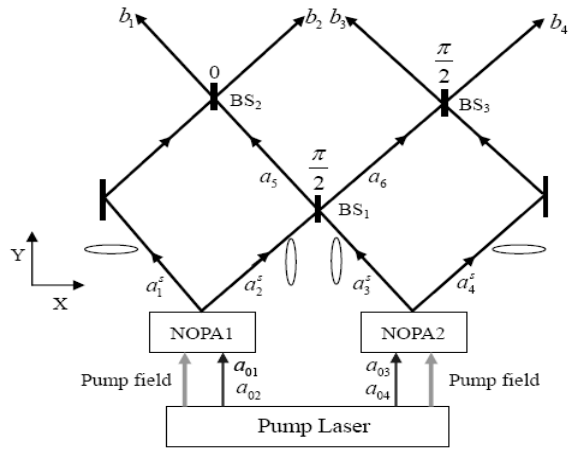


Fig.1 Principle schematic for CV quadripartite linear cluster state generation

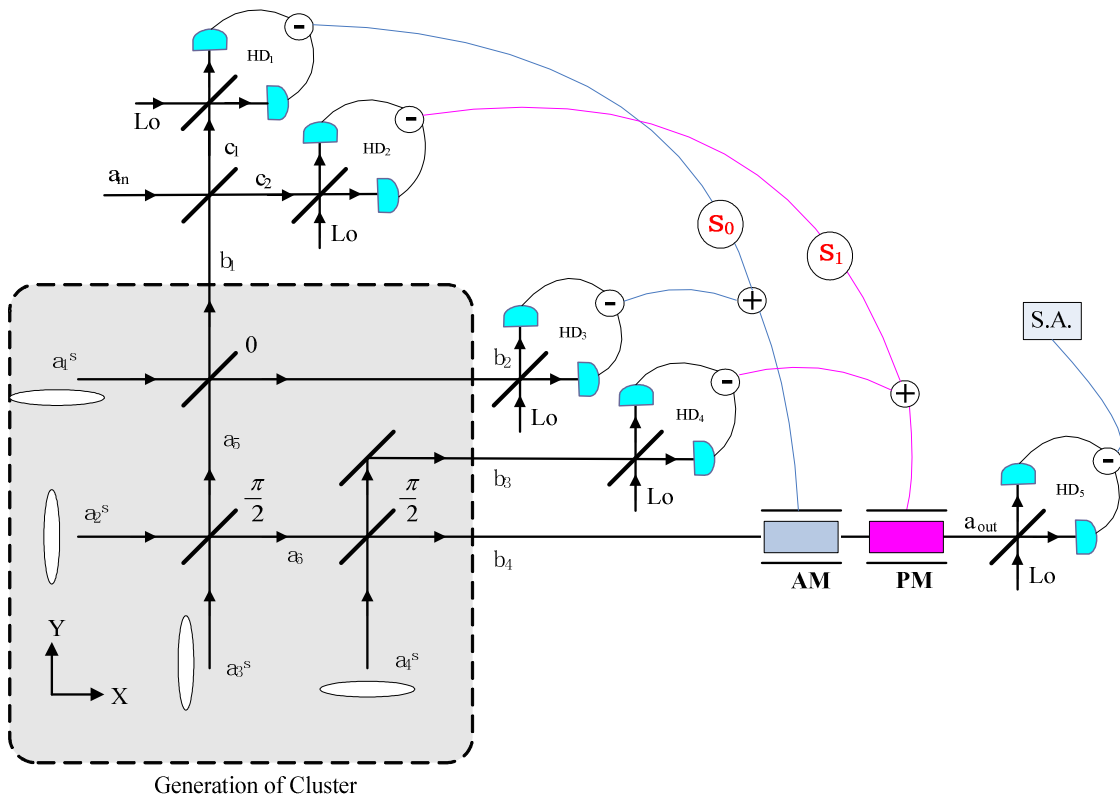


Fig.2 The experimental scheme to realize phase-space displacement operation using quadripartite linear cluster states

PM is a phase modulator; AM is a amplitude modulator; Lo is local oscillator.

s_0 and s_1 are the values subtracted from the measurement results

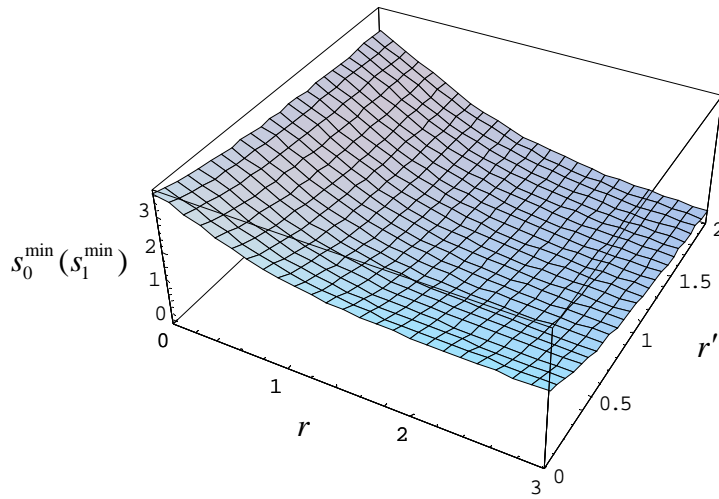


Fig. 3 Distinguishable displacement vs the initial squeezing parameter r of the Cluster state and the squeeze parameter r' of the input state

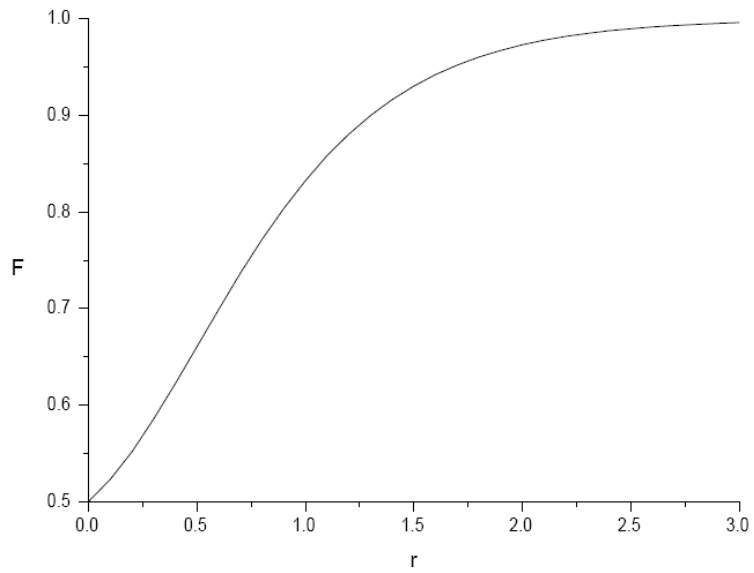


Fig. 4 The fidelity F vs the initial squeezing parameter r

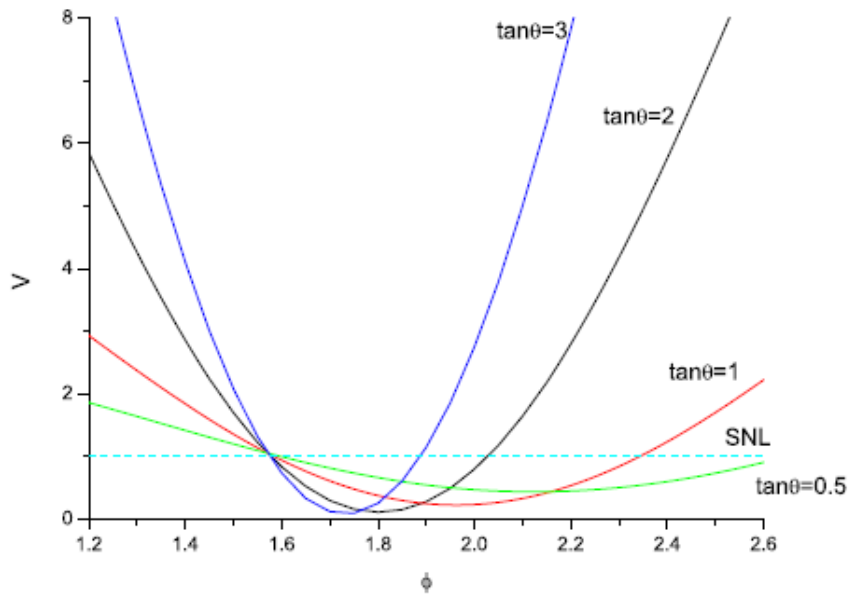


Fig.5 Fluctuation variances of the output mode $V(Y^{out} \sin \phi + X^{out} \cos \phi)$ vs phase difference ϕ of the HD₅ for the different detection phase θ . The dash line is the normalized shot noise limit (SNL), and taking $r = 2$

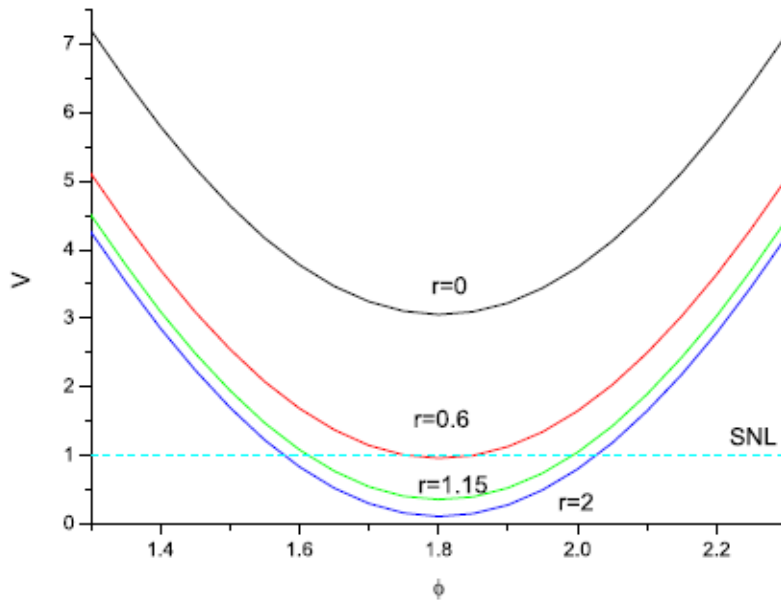


Fig.6 Fluctuation variances of the output mode $V(Y^{out} \sin \phi + X^{out} \cos \phi)$ vs phase difference ϕ of the HD₅ for the different squeezing factor r . The dash line is the normalized shot noise limit (SNL), and taking $\tan \theta = 2$

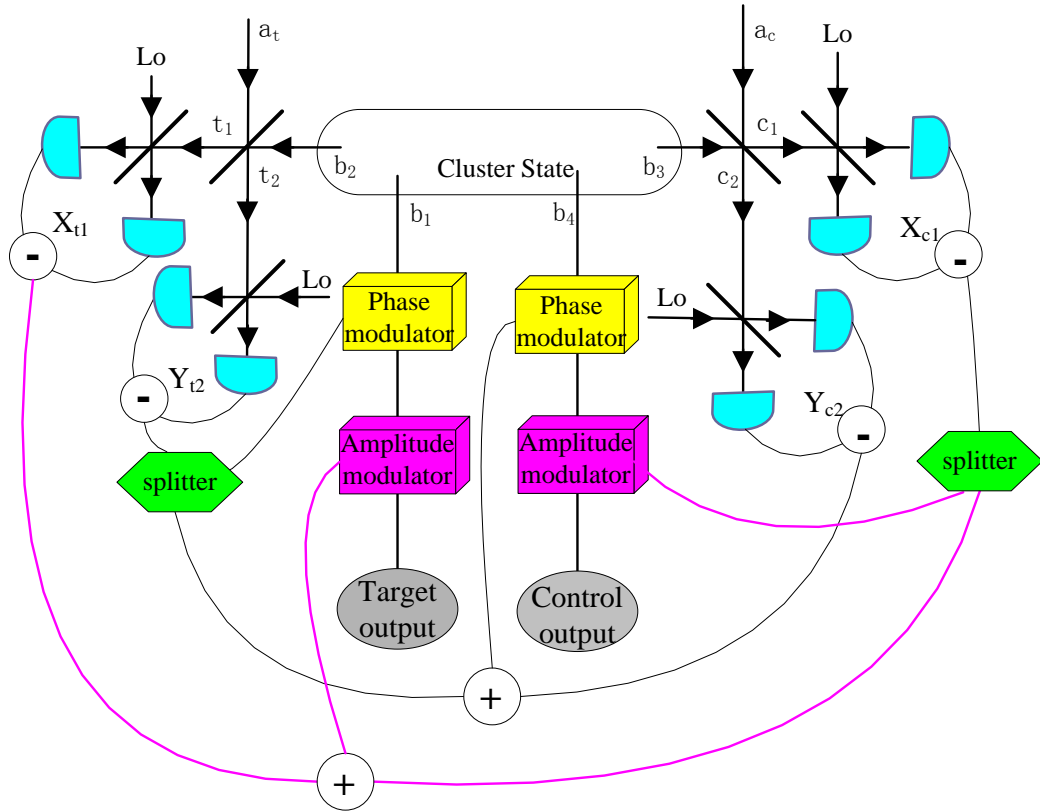
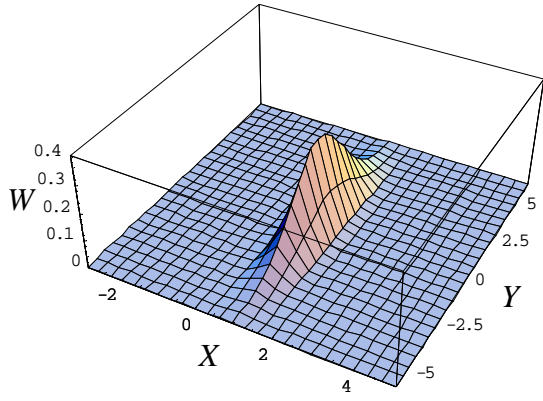
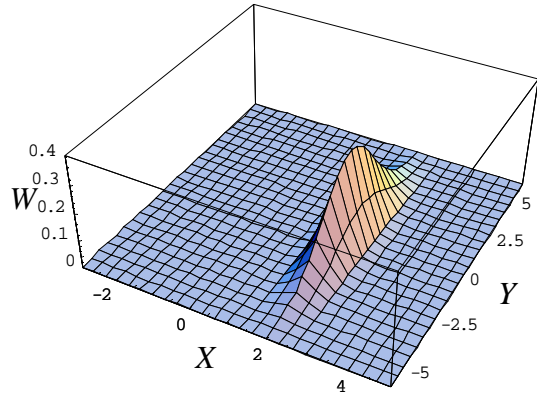


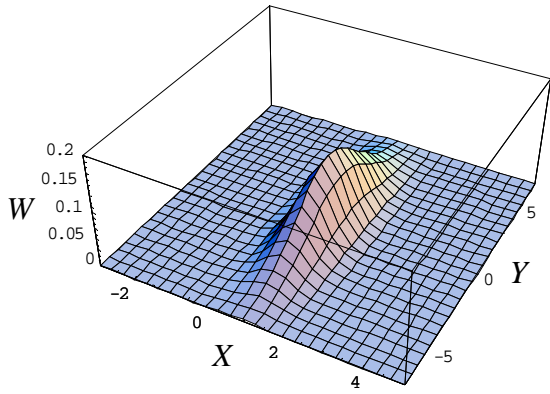
Fig. 7 Experiment scheme for realizing CV CNOT operation using linear quadripartite Cluster state.



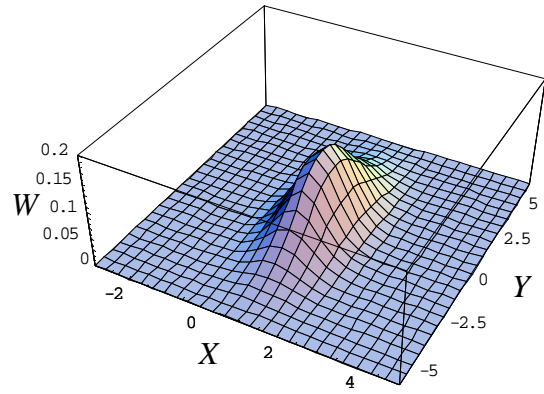
For Control input signal ($\sigma_x = e^{-1}, \sigma_y = e^1$)



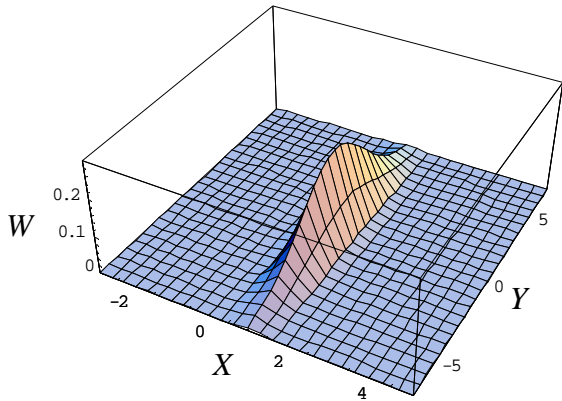
For Target input signal ($\sigma_x = e^{-1}, \sigma_y = e^1$)



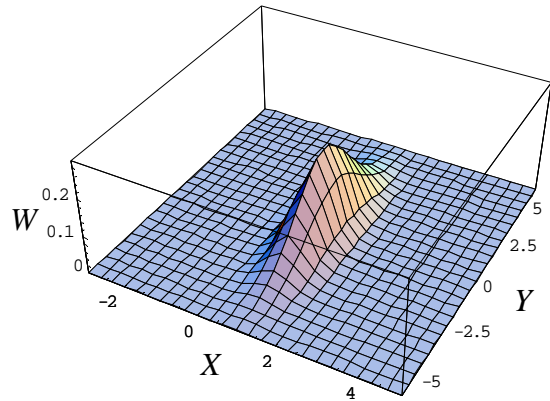
For Control output signal ($r = 1$)



For Target output signal ($r = 1$)



For Control output signal ($r = 3$)



For Target output signal ($r = 3$)

Fig. 8 Wigner functions $W(X, Y)$ of the input signals and output signals

X, Y are the amplitude and phase quadrature in the phase space